IEEE Access
Multidisciplinary | Rapid Review | Open Access Journal

Received August 25, 2021, accepted September 7, 2021, date of publication September 23, 2021, date of current version October 5, 2021.

Digital Object Identifier 10.1109/ACCESS.2021.3115143

Surface Routing for Wireless Power Transfer Using 2-D Relay Resonator Arrays

MASAHIRO MORITA, TAKUYA SASATANI, (Member, IEEE), RYO TAKAHASHI, AND YOSHIHIRO KAWAHARA, (Member, IEEE)
Graduate School of Engineering, The University of Tokyo, Tokyo 113-8656, Japan

Corresponding author: Masahiro Morita (morita@akg.t.u-tokyo.ac.jp)

This work was supported by the Japan Science and Technology Agency (JST), Exploratory Research for Advanced Technology (ERATO) under Grant JPMJER1501.

ABSTRACT Wireless power transfer via magnetic resonance coupling offers the prospect of autonomously charging connected devices. Previous work demonstrated that the system deployment can be facilitated by ''routing'' power on 2-D relay resonator arrays, using the multi-hop phenomenon. Power propagates through untethered relay resonators in such systems, and the routing strategy significantly affects the power transfer efficiency. However, most previous studies limit the routing to line-shaped routes, which compromises power transfer efficiency to preserve the simplicity of analysis. Here we show a surface routing approach, which can be orderly generated and is more efficient than linear routing. The confronting challenge is the complex representation of cross-coupled relays, which this work overcomes by conditioning the resonators' current by appending additional loading conditions to the relays. Simulation-based evaluations show that the proposed approach improves the efficiency by up to 10% in 1.5 m range power delivery.

INDEX TERMS Magnetic resonance coupling, multihop, power routing, wireless power transfer.

I. INTRODUCTION

Advancements in networking and battery technologies have accelerated the deployment of connected devices such as smartphones, tablets, and activity trackers. However, the need for wired and manual charging is hindering the utility of these devices. Wireless power transfer (WPT) via magnetic resonance coupling, which introduces resonant conditions to inductive WPT (*e.g.,* Qi) for enhancing misalignment tolerance, offers the promise for unaided charging experiences [1], [2]. Unlike competing approaches (*e.g.,* microwave, laser), this technology can safely deliver large amounts of power even when people are nearby [3]–[11]. However, it is still challenging to achieve autonomous charging experiences because of its narrow powering range.

Because mobile devices are frequently placed on tables, walls, and floors, augmenting these surfaces with wireless charging functions will eliminate manual charging. Thus, previous studies densely arranged transmitters on surfaces to achieve 2-D WPT [12]–[20]. However, the deployment of these systems is still challenging because they require custom-designed systems for each particular use case. A recent study presented Alvus, a reconfigurable 2-D WPT system that users can easily introduce by setting down untethered relay modules [See Fig. 1] [21]. This system utilizes the multi-hop phenomenon [22]–[29]; power propagates through the *passive* relay modules placed between the transmitter and the receiver, enabling power transfer within larger surfaces. By programming the state (*e.g.,* ON, OFF) of each relay module, Alvus can dynamically configure the ''virtual'' power paths on the surface [See Fig. 2(a) and Fig. 3(a)].

The routing strategy significantly affects the power transfer efficiency in WPT systems using 2-D resonator arrays. Most previous studies use ''linear routing,'' which connects the shortest route from the transmitter to the receiver [21], [30]–[32]. Although this approach is intuitive and preserves the simplicity of analysis, it limits the solution space and compromises power transfer efficiency. Thus, several studies lifted the restriction of linear routes and explored arbitrary surface routes that achieve higher efficiency [31]. However, the broad solution space makes random searching of such routes infeasible, and the cross-coupling effect makes the system analysis complex [33]–[35]. As an example of a technique based on similar physics, some studies develop wave devices inspired by metamaterials [36], designed to accommodate magneto-inductive waves in an array of coupled resonators forming a surface [26], [27], [37]. These works heuristically figure out the excitation condition that

The associate editor coordinating the review of this manuscript and approving it for publication was Martin Reisslein.

prevents null zones of power delivery. Furthermore, it is difficult to vary the dimensions of such arrays. Some approaches attempt to control these wave devices by making the components tunable [38], [39]; however, these approaches still require an exhaustive search for finding an optimal operating condition. At the system level, peripheral technologies for 2-D WPT systems based on resonator arrays have also been explored. One intensely explored direction is the localization techniques of the receiver placed on a 2-D relay resonator array [32], [40].

In this work, we show a orderly generated "surface routing" approach that achieves higher efficiency than the "linear routing" [See Fig. 2(b) and Fig. 3(b)]. The key to overcoming the challenge caused by the cross-coupling effect is adding the relays' loading condition so that the relay modules' current distribution becomes easily analyzable. This modification adds two more loading conditions to the relays, which can be implemented in reality by replacing the discrete switches of the previous implementation. These system modifications and the route generation rule based on the developed theory guarantees a higher efficiency without losing feasibility. To summarize, the contributions of this study are as follows:

- The proposal of an efficient and orderly built "surface routing" approach for WPT systems based on 2-D relay resonator arrays.
- An analysis of the constructed route and the discussion of applicable situations.
- Simulation-based evaluation of the power transfer efficiency that the proposed "surface routing" approach can achieve.

The following sections first present the fundamental idea of the proposed surface routing and the in-depth theoretical analysis underpinning the concept. Then, the proposed approach is evaluated through simulations, and finally, discussions and possible directions for future work are provided.

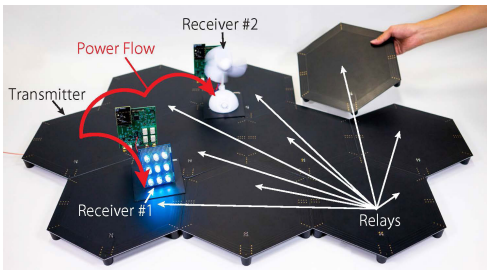

FIGURE 1. Overview of Alvus, a wireless power transfer system with a 2-D relay resonator array [21].

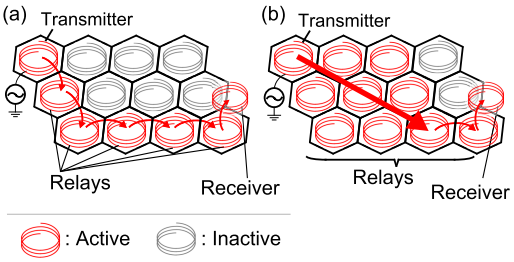

FIGURE 2. The overview of power route with relay resonator coils. (a) Linear route (Previous method [21]). (b) Surface route (Proposed method).

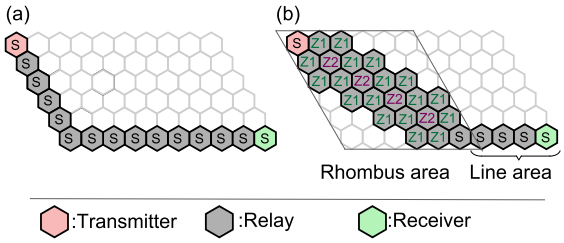

FIGURE 3. (a) Linear route (previous method [21]). (b) Surface route (Proposed method). White-filled modules represent the **OPEN** state. **S** represents the **SHORT** state, and **Z1** and **Z2** represent the new additional states.

II. THEORY

A. OVERVIEW

This section presents a theoretical analysis of the proposed "surface routing" approach. Our analysis assumes the WPT system presented in [21], which is based on 2-D relay resonator arrays. A straightforward "surface routing" results in cross-coupling, which exposes challenges in terms of system complexity. This paper overcomes this challenge through a two-fold approach. First, the powering route is divided into a rhombus area and a line area [see Fig. 3(b)]. Then, the focus shifts to the relays composing the rhombus area, which causes cross-coupling. Herein, we investigate the loading conditions of these relays that simplifies analysis. Particularly, we aim to simplify the analysis of relay current by adding the extra loading conditions (**Z1**, **Z2**) to the two states that relays in previous work possessed (**SHORT**, **OPEN**) [see Fig. 4].

This paper next proceeds to the description of the system and the details of the relay modification.

B. MODEL OF 2-D RELAY RESONATOR ARRAYS

Fig. 5 shows the equivalent circuit of a multi-hop WPT system with linear routing. The transmitter is connected to an AC power source with an operation frequency of f_0. Because the resonator modules are identical, the mutual inductance between adjacent resonators $-M$ ($M > 0$) and the copper loss of the resonator coils r are considered to be uniform. The mutual inductance between non-adjacent resonators can be ignored because the distances between them are sufficiently large [21]. Furthermore, resonators in the OFF state can be ignored because no current flows through them.

Extending investigation to routes that form a surface (*i.e.,* thick line, see Fig. 3(b)) could improve the power transfer efficiency because the search space will be extended. However, the non-uniform current distribution derived from the complex coupling between adjacent resonators (*i.e.,* cross-coupling) makes the expression of the system complex.

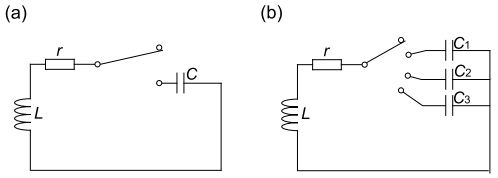

FIGURE 4. (a) Switching **SHORT** and **OPEN** (previous method) and (b) switching four required states of impedance (proposed method).

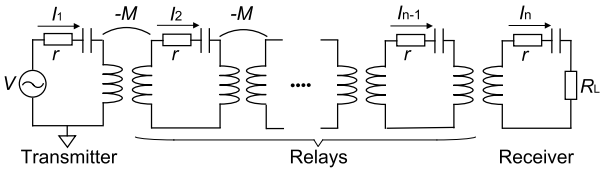

FIGURE 5. Equivalent circuit of a wireless power transfer system with a 2-D relay resonator array.

A naive approach towards finding an efficient route is to calculate the power transfer efficiency for all possible configurations. However, this method is infeasible because of the high computational cost. When surface routes are permitted, the number of possible resonator array states exponentially increases with the number of resonators because each can select its state independently. For example, the Alvus system [21] requires more than 160 modules to cover a 3 m × 3 m area, and this involves the evaluation of more than $2^{160} \simeq 10^{48}$ possible routes for an exhaustive search.

C. BUILDING EASILY EXPRESSED SURFACE ROUTES

Our key idea for achieving easily expressed surface routes is to make the current of symmetrically placed relay modules identical. This symmetry will reduce the number of variables used to express the system and make the analysis simple. The presented approach extends the powering route to "surface routes" (*i.e.,* thicker routes), as shown in Fig. 3(b). The area from the transmitter to the receiver is divided into a rhombus-shaped area and a remaining area. Herein, the line-shaped route in the rhombus-shaped area is replaced with a thicker line using 2 or 3 modules.

1) FORMULATION OF THE SYSTEM

The loading states of the relays are defined by the connected impedance z_i. The previous study used two-way switches to change between the **OPEN** and **SHORT** states. The proposed approach uses four-way switches to transit between the four states of impedances (*i.e.,* states) expressed as

$$z_i = \begin{cases} \infty, & OPEN(O) \\ r, & SHORT(S) \\ r + \mathrm{j}\omega M, & Z1 \\ r + 2\mathrm{j}\omega M, & Z2, \end{cases} \tag{1}$$

where ω is the operating angular frequency. In addition to **OPEN (O)** and **SHORT (S)** states, the **Z1** and **Z2** states, which are derived from the analysis presented in Section II-D and II-E, are introduced. In practice, these

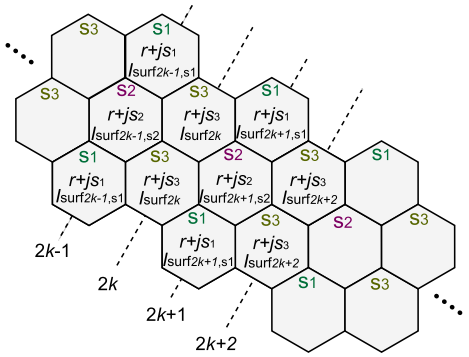

FIGURE 6. Geometric classification of resonators in the rhombus area. In each module, assigned state based on geometric classification (top), the definition of impedance (middle), and current of resonators (bottom) are described.

loading conditions can be implemented by connecting capacitors to the resonant coil via a four-way switch as shown in Fig. 4.

By applying Kirchhoff's Voltage Law (KVL) to the transmitter (equation 2), relay (equation 3), and receiver (equation 4), the following equations can be obtained:

$$V = z_1 I_1 - \sum_{k \in A_1} \mathrm{j}\omega M I_k \tag{2}$$

$$0 = z_i I_i - \sum_{k \in A_i} \mathrm{j}\omega M I_k \qquad (2 \le i < n) \tag{3}$$

$$0 = (z_n + R_L) I_n - \sum_{k \in A_n} \mathrm{j}\omega M I_k, \tag{4}$$

where V is the input voltage, R_L is the load resistance of the receiver, and A_i is the set of modules adjacent to module i. In addition, the power transfer efficiency of the system is expressed as follows:

$$\eta = \frac{P_R}{P_R + \sum_{k=1}^{n} P_{r_k}} = \frac{|I_n|^2 R_L}{|I_n|^2 R_L + \sum_{k=1}^{n} |I_k|^2 r} \tag{5}$$

The power transfer efficiency of WPT systems is known to be dependent on the load impedance R_L. A specific load value that maximizes the power transfer efficiency η is called the optimal load $R_{L_{opt}}$, which gives the maximum power transfer efficiency of the channel η_{opt}. In recent years, load impedance control techniques for actively tracking maximum efficiency conditions have been intensively studied [10]. Thus, the objective of this study is to increase η_{opt} by exploring new routing techniques that do not require heuristic explorations or exhaustive searching.

D. ANALYSIS OF UNIFORM CURRENT CONDITIONS

This paper next analyzes the conditions of **Z1** and **Z2** shown in equation (1), which gives a uniform current distribution.

Based on symmetry, the impedance of each relay is assigned as shown in Fig. 6 and we derive the appropriate impedance values of the three states, **S1**, **S2**, and **S3** herein. Because increasing the real impedance of the resonator causes power loss, it should be minimized to the internal

resistance of the coil, which cannot be eliminated. Thus, the real parts of all three states should be equal to the internal resistance of the coil, r. Here, we define the imaginary impedances of these three states **S1**, **S2**, and **S3** as js_1, js_2, and js_3, respectively.

To make the current distribution uniform, the values of $I_{surf\,2k+1,s1}$ and $I_{surf\,2k+1,s2}$ $(k = 1, 2, 3\ldots)$ in Fig. 6 need to be equal. By applying KVL to the resonators indicated by the current values of $I_{surf\,2k+1,s1}$ and $I_{surf\,2k+1,s2}$, the following equations are obtained:

$$\begin{aligned} 0 &= (r+\mathrm{j}s_1)I_{surf\,2k+1,s1} - \mathrm{j}\omega M(I_{surf\,2k+1,s2} + I_{surf\,2k} + I_{surf\,2k+2}) \\ 0 &= (r+\mathrm{j}s_2)I_{surf\,2k+1,s2} - 2\mathrm{j}\omega M(I_{surf\,2k+1,s1} + I_{surf\,2k} + I_{surf\,2k+2}). \end{aligned} \tag{6}$$

The following equation is obtained from above two equations:

$$\frac{I_{surf\,2k+1,s2}}{I_{surf\,2k+1,s1}} = \frac{1 + \frac{s_1}{\omega M} - \frac{\mathrm{j}}{\alpha}}{1 + \frac{s_2}{2\omega M} - \frac{\mathrm{j}}{2\alpha}} \tag{7}$$

$$\alpha = \frac{\omega M}{r}, \tag{8}$$

where α, called the kQ product, positively correlates with power efficiency in single-hop systems (WPT systems without relay resonators) and is typically larger than 1 in such systems. The kQ product between two series LC resonators with resistance r_1 and r_2 is the follows:

$$\alpha_{1,2} = \frac{\omega M_{1,2}}{\sqrt{r_1 r_2}}, \tag{9}$$

where $M_{1,2}$ is the mutual inductance between the two resonators. The measured kQ product between two adjacent resonators used in the previous implementation [21] was larger than 10. Therefore, the value of $\frac{1}{\alpha}$ in equation (7) can be ignored, and $I_{surf\,2k+1,s1}$ and $I_{surf\,2k+1,s2}$ can be approximated to be identical by introducing the following relationship:

$$s_2 = 2s_1. \tag{10}$$

Now, $I_{surf\,2k+1}$ is used instead of $I_{surf\,2k+1,s1}$ and $I_{surf\,2k+1,s2}$.

E. DETERMINING THE LOADING CONDITIONS

For ensuring that the presented surface routing approach is more efficient than linear routing, the impedance repertoire is defined so that the two approaches (*i.e.,* the proposed surface routing and the previously used linear routing) can be easily compared. By applying KVL to the resonators of the surface routing whose current values are expressed as $I_{surf\,2k}$ and $I_{surf\,2k+1}$, the following equation is obtained.

$$\begin{cases} 0 = (r + \mathrm{j}s_3 - \mathrm{j}\omega M)I_{\mathrm{surf}_{2k}} - 2\mathrm{j}\omega M(I_{\mathrm{surf}_{2k-1}} + I_{\mathrm{surf}_{2k+1}}) \\ 0 = (r + \mathrm{j}s_1 - \mathrm{j}\omega M)I_{\mathrm{surf}_{2k+1}} - \mathrm{j}\omega M(I_{\mathrm{surf}_{2k}} + I_{\mathrm{surf}_{2k+2}}) \end{cases} \tag{11}$$

The KVL of the linear routing is as follows:

$$\begin{cases} 0 = rI_{\mathrm{line}_{2k}} - \mathrm{j}\omega M(I_{\mathrm{line}_{2k-1}} + I_{\mathrm{line}_{2k+1}}) \\ 0 = rI_{\mathrm{line}_{2k+1}} - \mathrm{j}\omega M(I_{\mathrm{line}_{2k}} + I_{\mathrm{line}_{2k+2}}), \end{cases} \tag{12}$$

where N modules from module 1 to module N form a line and the current value of the i^{th} module is defined as I_{line_i}.

To easily compare equation (11) and equation (12), let s_1 and s_3 be defined as follows:

$$s_1 = s_3 = \omega M. \tag{13}$$

Then, equation (11) can be transformed into the following:

$$\begin{cases} 0 = rI_{\mathrm{surf}_{2k}} - 2\mathrm{j}\omega M(I_{\mathrm{surf}_{2k-1}} + I_{\mathrm{surf}_{2k+1}}) \\ 0 = rI_{\mathrm{surf}_{2k+1}} - \mathrm{j}\omega M(I_{\mathrm{surf}_{2k}} + I_{\mathrm{surf}_{2k+2}}) \end{cases} \tag{14}$$

Because equation (12) and equation (14) look similar, the two routes can now be easily compared. As a result, **S1** and **S3** correspond to **Z1** and **S2** corresponds to **Z2**. Thereby, the impedance expressed as **Z1** and **Z2** in equation (1) is now derived. Next, we proceed to analyze the power transfer efficiency using these loading conditions.

III. THEORETICAL ANALYSIS OF POWER EFFICIENCY

In this section, theoretical analysis is performed to show that the proposed surface routing approach obtains higher efficiency than linear routing. We conduct this analysis in two steps using the tentative linear route model shown in Fig. 7(b), which is a linear resonator array system consisting of N modules. First, it is proved that the surface route shown in Fig. 7(a) is more efficient than the tentative linear route shown in Fig. 7(b). Next, it is proved that the tentative linear route shown in Fig. 7(b) is more efficient than the linear route shown in Fig. 7(c). Consequently, we can confirm that the surface route is theoretically more efficient than the former linear routing.

A. THE SURFACE ROUTE AND THE TENTATIVE LINEAR ROUTE

Fig. 7(a) shows the circuit model of the surface route (Fig. 3(b)), where modules are arranged in n columns in the rhombus area and the receiver module is in column N. The value annotated in each module is the impedance of the module. The KVL of each module in Fig. 7(a) can be expressed as the following:

- Transmitter:

$$V = rI_{\mathrm{surf}_1} - 2\mathrm{j}\omega M I_{\mathrm{surf}_2}$$

- Relay in the 2[nd] column:

$$0 = rI_{\mathrm{surf}_2} - \mathrm{j}\omega M(I_{\mathrm{surf}_1} + 2\,I_{\mathrm{surf}_3})$$

- Relays between the 3[rd] and $(n-2)^{\mathrm{th}}$ column:

$$\begin{cases} 0 = rI_{\mathrm{surf}_k} - \mathrm{j}\omega M(I_{\mathrm{surf}_{k-1}} + I_{\mathrm{surf}_{k+1}}), & k : odd \\ 0 = rI_{\mathrm{surf}_k} - 2\mathrm{j}\omega M(I_{\mathrm{surf}_{k-1}} + I_{\mathrm{surf}_{k+1}}), & k : even \end{cases}$$

- Relay in the $n-1^{\mathrm{th}}$ column:

$$0 = rI_{\mathrm{surf}_{n-1}} - \mathrm{j}\omega M(2\,I_{\mathrm{surf}_{n-2}} + I_{\mathrm{surf}_n})$$

- Relay in the n^{th} column:

$$0 = rI_{\mathrm{surf}_n} - \mathrm{j}\omega M(2\,I_{\mathrm{surf}_{n-1}} + I_{\mathrm{surf}_{n+1}})$$

- Relays between the $n+1^{\mathrm{th}}$ and the $N-1^{\mathrm{th}}$ column:

$$0 = rI_{\mathrm{surf}_k} - \mathrm{j}\omega M(I_{\mathrm{surf}_{k-1}} + I_{\mathrm{surf}_{k+1}})$$

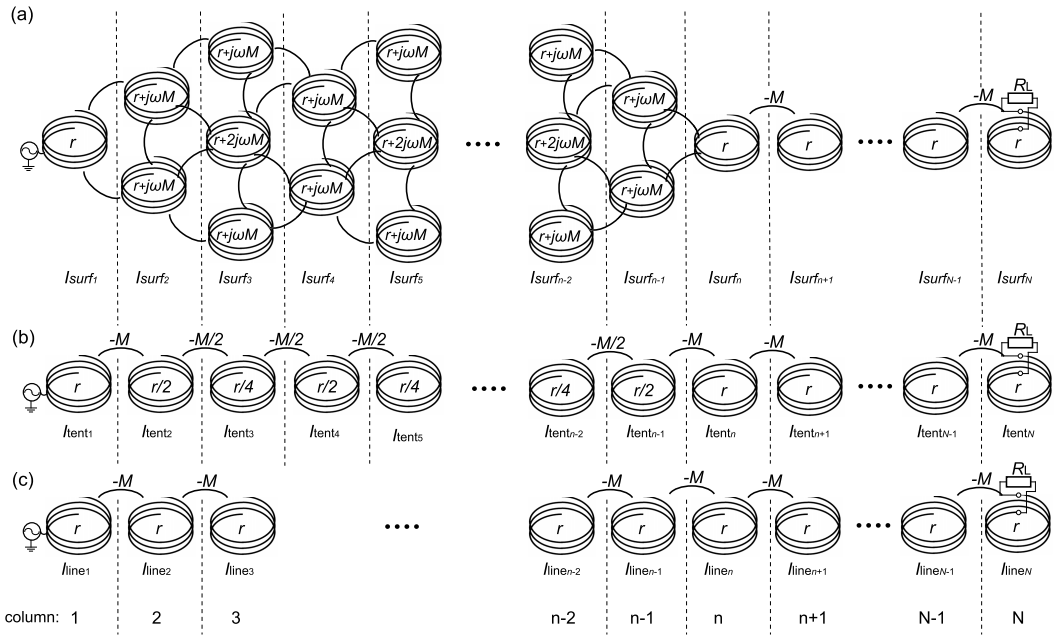

FIGURE 7. (a) Proposed surface route. (b) Tentative circuit of the linear relay resonator array. (c) Linear route (previous method [21]). In each module, the impedance is described. Each current value is described under the module.

- Relay in the N^{th} column

$$0 = (r + R_L)I_{\text{surf}_N} - \text{j}\omega M I_{\text{surf}_{N-1}}$$

These equations can be reorganized as follows:

$$\boldsymbol{V} = \boldsymbol{Z_0 I_{\text{surf}}}, \tag{15}$$

where

$$\boldsymbol{V} = \left[V, 0, 0, \ldots, 0, 0\right]^{\text{T}} \tag{16}$$

$$\boldsymbol{Z_0} = \begin{bmatrix} \boldsymbol{Z_{11}} & \boldsymbol{Z_{12}} \\ \boldsymbol{Z_{21}} & \boldsymbol{Z_{22}} \end{bmatrix} \tag{17}$$

$$\boldsymbol{Z_{11}} = \begin{bmatrix} r & -\text{j}\omega M & 0 & \cdots & \cdots & \cdots & \cdots & 0 \\ -\text{j}\omega M & \frac{r}{2} & \frac{-\text{j}\omega M}{2} & \ddots & & & & \vdots \\ 0 & \frac{-\text{j}\omega M}{2} & \frac{r}{4} & \frac{-\text{j}\omega M}{2} & \ddots & & & \vdots \\ \vdots & \ddots & \frac{-\text{j}\omega M}{2} & \frac{r}{2} & \frac{-\text{j}\omega M}{2} & \ddots & & \vdots \\ \vdots & & \ddots & \ddots & \ddots & \ddots & \ddots & \vdots \\ \vdots & & & \ddots & \frac{-\text{j}\omega M}{2} & \frac{r}{4} & \frac{-\text{j}\omega M}{2} & 0 \\ \vdots & & & & \ddots & \frac{-\text{j}\omega M}{2} & \frac{r}{2} & -\text{j}\omega M \\ 0 & \cdots & \cdots & \cdots & \cdots & 0 & -\text{j}\omega M & r \end{bmatrix} \tag{18}$$

$$\boldsymbol{Z_{22}} = \begin{bmatrix} r & -\text{j}\omega M & 0 & \cdots & \cdots & \cdots & 0 \\ -\text{j}\omega M & r & -\text{j}\omega M & \ddots & & & \vdots \\ 0 & -\text{j}\omega M & r & -\text{j}\omega M & \ddots & & \vdots \\ \vdots & \ddots & \ddots & \ddots & \ddots & \ddots & \vdots \\ \vdots & & \ddots & -\text{j}\omega M & r & -\text{j}\omega M & 0 \\ \vdots & & & \ddots & -\text{j}\omega M & r & -\text{j}\omega M \\ 0 & \cdots & \cdots & \cdots & 0 & -\text{j}\omega M & r + R_L \end{bmatrix} \tag{19}$$

$$\boldsymbol{Z_{12}} = \begin{bmatrix} 0 & \cdots & \cdots & 0 \\ \vdots & & \ddots & \vdots \\ 0 & & & \\ -\text{j}\omega M & 0 & \cdots & 0 \end{bmatrix} \tag{20}$$

$$\boldsymbol{Z_{21}} = \begin{bmatrix} 0 & \cdots & 0 & -\text{j}\omega M \\ & & & 0 \\ \vdots & \ddots & & \vdots \\ 0 & \cdots & \cdots & 0 \end{bmatrix} \tag{21}$$

$$\boldsymbol{I_{\text{surf}}} = \begin{bmatrix} I_{\text{surf}_1} \\ 2\,I_{\text{surf}_2} \\ 4\,I_{\text{surf}_3} \\ 2\,I_{\text{surf}_4} \\ 4\,I_{\text{surf}_5} \\ \vdots \\ 2\,I_{\text{surf}_{n-3}} \\ 4\,I_{\text{surf}_{n-2}} \\ 2\,I_{\text{surf}_{n-1}} \\ I_{\text{surf}_n} \\ I_{\text{surf}_{n+1}} \\ \vdots \\ I_{\text{surf}_{N-1}} \\ I_{\text{surf}_N} \end{bmatrix}. \tag{22}$$

V and I_{surf} are N-dimensional vectors, Z_0 is a $N \times N$ matrix, Z_{11} is a $n \times n$ matrix, Z_{22} is a $(N-n) \times (N-n)$ matrix, Z_{12} is a $n \times (N-n)$ matrix and Z_{21} is a $(N-n) \times n$ matrix.

As for the tentative linear route shown in Fig. 7(b), the following equation is established:

$$\boldsymbol{V} = \boldsymbol{Z_0 I_{\text{tent}}}, \tag{23}$$

where

$$\boldsymbol{I_{\mathbf{tent}}} = \left[I_{\mathrm{tent}_1}, I_{\mathrm{tent}_2}, I_{\mathrm{tent}_3} \ldots I_{\mathrm{tent}_{n-1}}, I_{\mathrm{tent}_n}, I_{\mathrm{tent}_{n+1}}, \ldots, I_{\mathrm{tent}_N}\right]^{\mathrm{T}}. \tag{24}$$

When the load values (R_L) of the surface route (Fig. 3(a)) and the tentative linear route (Fig. 3(b)) are equal, both $\boldsymbol{Z_0}$ in equation (15) and equation (23) are the same. Because $\boldsymbol{Z_0}$ is a full-rank square matrix, the following equation is obtained from equation (15) and (23):

$$\boldsymbol{Z_0}^{-1}\boldsymbol{V} = \boldsymbol{I_{\mathbf{surf}}} = \boldsymbol{I_{\mathbf{tent}}} \tag{25}$$

From this and equation (22), the total power loss of the surface route (Fig. 7(a)) is

$$P_{\mathrm{surf}_{\mathrm{loss}}} = |I_{\mathrm{surf}_1}|^2 r + \sum_{k=1}^{\frac{n-3}{2}} \left(2|I_{\mathrm{surf}_{2k}}|^2 r + 3|I_{\mathrm{surf}_{2k+1}}|^2 r\right) + 2|I_{\mathrm{surf}_{n-1}}|^2 r + |I_{\mathrm{surf}_n}|^2 r + P_{\mathrm{common}}, \tag{26}$$

where

$$P_{\mathrm{common}} = \sum_{i=n+1}^{N} \left(|I_{\mathrm{surf}_i}|^2 r\right) + |I_{\mathrm{surf}_N}|^2 R_L$$

The total power loss of the tentative linear route (Fig. 7(b)) is the following:

$$P_{\mathrm{tent}_{\mathrm{loss}}} = |I_{\mathrm{surf}_1}|^2 r + \sum_{k=1}^{\frac{n-3}{2}} \left(2|I_{\mathrm{surf}_{2k}}|^2 r + 4|I_{\mathrm{surf}_{2k+1}}|^2 r\right) + 2|I_{\mathrm{surf}_{n-1}}|^2 r + |I_{\mathrm{surf}_n}|^2 r + P_{\mathrm{common}}. \tag{27}$$

Therefore, the following relationship holds:

$$P_{\mathrm{surf}_{\mathrm{loss}}} < P_{\mathrm{tent}_{\mathrm{loss}}} \tag{28}$$

Equation (28) holds for any load impedance value. According to equation (25), the load current in the surface route and the load current in the tentative linear route are the same, which means that the power consumed in the load is equal. The energy loss and the power transfer efficiency are negatively correlated when the power delivered to the load is constant. Therefore, the following equation holds:

$$\eta_{\mathrm{tent}}(R_L) < \eta_{\mathrm{surf}}(R_L), \tag{29}$$

where $\eta_{\mathrm{surf}}(R)$ is the power transfer efficiency in the surface route and $\eta_{\mathrm{line}}(R)$ is the power transfer efficiency in the tentative linear route. Equation (29) holds for any value of R_L, which shows that

$$\eta_{\mathrm{tent}_{\mathrm{opt}}} < \eta_{\mathrm{surf}_{\mathrm{opt}}}, \tag{30}$$

where $\eta_{\mathrm{surf}_{\mathrm{opt}}}$ is the maximum power transfer efficiency in the surface route and $\eta_{\mathrm{tent}_{\mathrm{opt}}}$ is the maximum power transfer efficiency in the tentative linear route.

B. THE LINEAR ROUTE AND THE TENTATIVE LINEAR ROUTE

Fig. 7(c) shows the linear route used in former work. The kQ product between adjacent resonators of the tentative linear route is $\sqrt{2}\alpha$ in the rhombus-shaped area and is α in the line area, while that of the linear route is uniformly α.

Thereby, the power transfer efficiency of the tentative linear route (η_{tent}) and power transfer efficiency of the linear route (η_{line}) are expressed as follows using the parameter $\beta = \frac{R_L}{r}$ [see the appendix for details of the formulation]:

$$\eta_{\mathrm{tent}}(\beta) = \begin{cases} \left(1-\frac{1}{\beta}\right)^{\frac{N-n+1}{2}} \left(1-\frac{\beta}{\alpha^2}\right)^{\frac{N}{2}} \left(1-\frac{1}{2\beta}\right)^{\frac{n-1}{2}} \\ \qquad N : even \\ \left(1-\frac{1}{\beta}\right)^{\frac{N+1}{2}} \left(1-\frac{\beta}{\alpha^2}\right)^{\frac{N-n}{2}} \left(1-\frac{\beta}{2\alpha^2}\right)^{\frac{n-1}{2}} \\ \qquad N : odd \end{cases} \tag{31}$$

$$\eta_{\mathrm{line}}(\beta) = \begin{cases} \left(1-\frac{1}{\beta}\right)^{\frac{N}{2}} \left(1-\frac{\beta}{\alpha^2}\right)^{\frac{N}{2}}, & N : even \\ \left(1-\frac{1}{\beta}\right)^{\frac{N+1}{2}} \left(1-\frac{\beta}{\alpha^2}\right)^{\frac{N-1}{2}}, & N : odd. \end{cases} \tag{32}$$

By comparing equation (32) with equation (31), the following equation is obtained when the load impedance for both approaches are equal:

$$\eta_{\mathrm{line}}(\beta) < \eta_{\mathrm{tent}}(\beta) \tag{33}$$

The above equation holds at any positive value of β, implying that

$$\eta_{\mathrm{line}_{\mathrm{opt}}} < \eta_{\mathrm{tent}_{\mathrm{opt}}}, \tag{34}$$

where $\eta_{\mathrm{line}_{\mathrm{opt}}}$ is the maximum value of $\eta_{\mathrm{line}}(\beta)$ and $\eta_{\mathrm{tent}_{\mathrm{opt}}}$ is the maximum value of $\eta_{\mathrm{tent}}(\beta)$.

Finally, combining equations (30) and (34), the following can be obtained:

$$\eta_{\mathrm{line}_{\mathrm{opt}}} < \eta_{\mathrm{surf}_{\mathrm{opt}}} \tag{35}$$

Thus, when compared to linear routing approaches, the proposed surface routing improves the power transfer efficiency for any number of relays between the transmitter and the receiver.

IV. SIMULATION OF POWER EFFICIENCY

Finally, we evaluated the power transfer efficiency using the frequency response analysis of LTspice® [41], a circuit simulator distributed by Analog Devices. Fig. 8(a) shows the classification of a receiver position based on geometric symmetry. The transmitter is placed at the center position 'A,' the relay modules are densely packed around the transmitter, and the receiver is placed on any of the relays or the transmitter. The power transfer route and the obtained power transfer efficiency are determined from the positional relationship between the transmitter and receiver. Therefore, the receiver placement on the relay with the same colours can be treated as the same.

The simulation was performed using the previous linear route approach and the proposed surface routing approach.

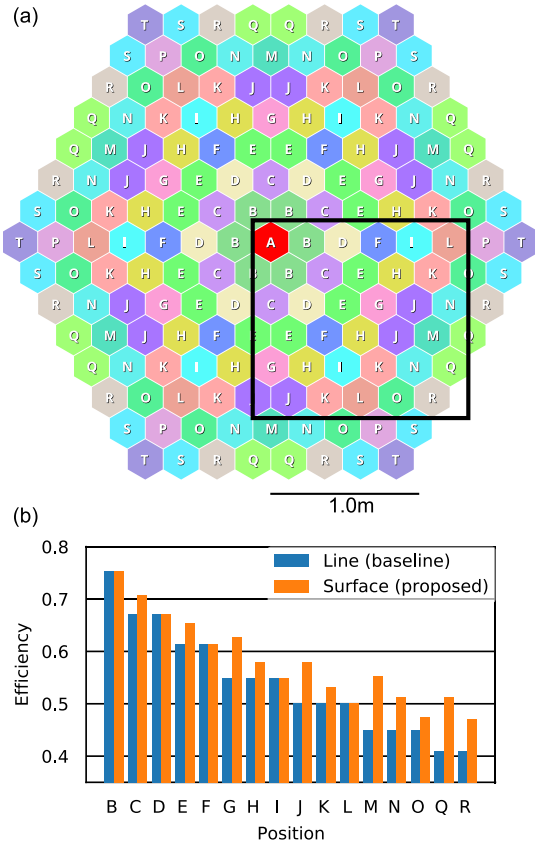

FIGURE 8. Receiver position and power transfer efficiency. (a) Geometric classification of the receiver position. The transmitter is located in 'A'. The same alphabet is assigned to receiver positions that cannot be distinguished geometrically from the transmitter. (b) Power transfer efficiency of the previous method ('line') and the proposed method ('surface') calculated by LTspice® [41] (circuit simulation software).

The kQ product between adjacent resonators was uniformly set to 10, including the coupling between the relay and the receiver. This value is based on measurements using resonators of the same size as the previous implementation [21]. Herein, the transmitter and relays are hexagonal with a diagonal distance of 25 cm and a receiver is 10 cm × 10 cm square. We set the operating frequency of the AC power source, the coupling coefficient between adjacent resonators, the copper loss of the resonator, and self-inductance of the resonator coil to 6.78 MHz, −0.1, 1.0 Ω, and 2.35 µF respectively in the simulation.

Fig. 8(b) shows the power transfer efficiency with various receiver positions obtained by the simulation. We placed the receiver within the 1.5 m × 1.4 m rectangular area marked with a black square in Fig. 8(a). The power transfer efficiency of the proposed method is higher than or equal to that of the previous linear routing approach in any position. For example, there is an 8% improvement in efficiency at the receiver position 'G' and a 10 % improvement at receiver positions of 'M' and 'Q.' We finally note as a limitation that when the receiver is positioned where the rhombus area does not exist and the route generated by the presented approach matches the line route (*e.g.*, 'B', 'D' and 'F'), the efficiency between the linear routing and the proposed routing obviously matches.

V. CONCLUSION

This work presented a ''surface routing'' approach, which is more efficient than ''linear routing'', which could be orderly generated because it preserves the simplicity of analysis. We overcame the underlying challenges caused by the complex representation of the cross-coupled relays, which results in a multi-body problem, by introducing new relay states determined by theory. Theoretical analysis revealed that the presented approach improves the power transfer efficiency compared to the former linear methods by up to 10%. These results were also confirmed through established evaluation approaches using circuit simulators. Furthermore, unlike other surface routing methods using 2-D relay resonator arrays, the presented surface route can be orderly generated and allows operation on a single frequency band.

This work improves the utility of wireless power transfer systems and pioneers a new research field of efficiently ''routing'' energy in inductive methods, which promises to empower future mobile computing systems. We note as a limitation that the route's search space is still limited to rhombus routes, and extending the solution space while enabling orderly route generation is a promising direction of future work.

APPENDIX

A. POWER TRANSFER EFFICIENCY OF LINEAR RESONATOR ARRAY CIRCUIT

The power transfer efficiency when N resonators are arranged in a straight line is described herein. The resonators are numbered from 1 to N in geometrical order. Resonator 1 is a power transmitter, resonator N is a receiver, and the rest are relay resonators. Only the mutual inductance between adjacent relays are taken into account: $M_{k,k+1} (0 \leq k < N)$. The resistance of the k^{th} resonator is r_k, and the resistance of the load is R_L. The power transfer efficiency η is expressed using the kQ product between the resonators.

The kQ product between the k^{th} resonator and $k + 1^{\text{th}}$ resonator is defined as follows:

$$\alpha_{k,k+1} = \frac{\omega M_{k,k+1}}{\sqrt{r_k r_{k+1}}}. \tag{36}$$

A set of coupled resonators can be regarded as a K impedance inverter [42], and thus

$$Z_{in(k)} = \begin{cases} r_k + \dfrac{(\omega M_{k,k+1})^2}{Z_{in(k+1)}}, & (1 \leq k < N) \\ r_N + R_L, & (k = N), \end{cases} \tag{37}$$

where $Z_{in(k)}$ is the input impedance of the k^{th} resonator. By using P_L, which represents the power consumed by the receiver load, and $P_{seq(k)}$, which represents the power consumed by the k^{th} and subsequent resonators, the power

transfer efficiency can be expressed as follows:

$$\eta = \frac{P_L}{P_{seq(1)}} = \frac{P_L}{P_{seq(N)}} \times \frac{P_{seq(N)}}{P_{seq(N-1)}} \times \frac{P_{seq(N-1)}}{P_{seq(N-2)}} \cdots \times \frac{P_{seq(2)}}{P_{seq(1)}} \quad (38)$$

The ratio of P_L to $P_{seq(N)}$ is equal to the ratio of R_L and $r_N + R_L$. The difference between $P_{seq(k+1)}$ and the power consumed by the $P_{seq(k)}$ is the power consumed by the resistance r_k of the k^{th} resonator. Hence, the power transfer efficiency is expressed as the following:

$$\eta = \frac{R_L}{Z_{in(N)}} \times \frac{Z_{in(N-1)} - r_{N-1}}{Z_{in(N-1)}} \times \cdots \times \frac{Z_{in(1)} - r_1}{Z_{in(1)}} \quad (39)$$

.

Here, A_k and β are defined as follows:

$$A_k = \frac{Z_{in(k)} - r_k}{Z_{in(k)}}, \quad (40)$$

$$\beta = \frac{R_L}{r_N}. \quad (41)$$

By using equation (37), the relationship between A_k and A_{k+1} $(k < N)$ is the follows:

$$A_k = \frac{1}{1 + \frac{1}{\alpha^2_{k,k+1}(1 - A_{k+1})}} \quad (42)$$

Next, we will prove that the following approximation holds when $\alpha_{i,i+1} \gg 1$, $\beta \gg 1$, and $\alpha^2_{i,i+1} \gg \beta$ $(1 \leq i < N)$:

$$A_i \simeq \begin{cases} 1 - \dfrac{\alpha^2_{i+1,i+2}\alpha^2_{i+3,i+4} \cdots \alpha^2_{N-1,N}}{\alpha^2_{i,i+1}\alpha^2_{i+2,i+3} \cdots \alpha^2_{N-2,N-1}\beta} \\ N - i : even \\ 1 - \dfrac{\alpha^2_{i+1,i+2}\alpha^2_{i+3,i+4} \cdots \alpha^2_{N-2,N-1}\beta}{\alpha^2_{i,i+1}\alpha^2_{i+2,i+3} \cdots \alpha^2_{N-3,N-2}\alpha^2_{N-1,N}} \\ N - i : odd. \end{cases} \quad (43)$$

First, we explain the case of $i = N$.

$$A_N = \frac{R_L}{r_N + R_L} = \frac{1}{1 + \frac{1}{\beta}} \simeq 1 - \frac{1}{\beta} \quad (44)$$

Therefore, equation (43) holds for $i = N$.

Suppose equation (43) holds for $i = k$, where $N - k$ is even. The following equation is derived from equation (42):

$$\begin{aligned} A_{k-1} &= \frac{1}{1 + \frac{1}{\alpha^2_{k-1,k}(1 - A_k)}} \\ &\simeq \frac{1}{1 + \frac{\alpha^2_{k,k+1}\alpha^2_{k+2,k+3} \cdots \alpha^2_{N-2,N-1}\beta}{\alpha^2_{k-1,k}\alpha^2_{k+1,k+2}\alpha^2_{k+3,k+4} \cdots \alpha^2_{N-1,N}}} \\ &\simeq 1 - \frac{\alpha^2_{k,k+1}\alpha^2_{k+2,k+3} \cdots \alpha^2_{N-2,N-1}\beta}{\alpha^2_{k-1,k}\alpha^2_{k+1,k+2}\alpha^2_{k+3,k+4} \cdots \alpha^2_{N-1,N}} \end{aligned} \quad (45)$$

Therefore, when equation (42) holds for the condition $k = i$, equation (42) holds even for the condition $k = i - 1$.

Similarly, when $N - k$ is odd, equation (43) holds for $i = k$.

$$\begin{aligned} A_{k-1} &= \frac{1}{1 + \frac{1}{\alpha^2_{k-1,k}(1 - A_k)}} \\ &\simeq \frac{1}{1 + \frac{\alpha^2_{k,k+1}\alpha^2_{k+2,k+3} \cdots \alpha^2_{N-3,N-2}\alpha^2_{N-1,N}}{\alpha^2_{k-1,k}\alpha^2_{k+1,k+2} \cdots \alpha^2_{N-2,N-1}\beta}} \\ &\simeq 1 - \frac{\alpha^2_{k,k+1}\alpha^2_{k+2,k+3} \cdots \alpha^2_{N-3,N-2}\alpha^2_{N-1,N}}{\alpha^2_{k-1,k}\alpha^2_{k+1,k+2} \cdots \alpha^2_{N-2,N-1}\beta} \end{aligned} \quad (46)$$

Therefore, when equation (43) holds for the condition of $k = i$, equation (43) holds even for the condition $k = i - 1$. Thus, by mathematical induction, equation (43) always holds.

Furthermore, equation (39) can also be represented as follows:

$$\eta = A_N \times A_{N-1} \times \cdots \times A_1. \quad (47)$$

Thereby, the power transfer efficiency can be expressed using the kQ product and the nondimensionalized load β as follows:

$$\eta \simeq \left(1 - \frac{1}{\beta}\right) \times \left(1 - \frac{\beta}{\alpha^2_{N-1,N}}\right) \times \cdots \times \left(1 - \frac{\alpha^2_{1,2} \cdots \alpha^2_{N-2,N-1}\beta}{\alpha^2_{2,3} \cdots \alpha^2_{N-1,N}}\right) \quad (48)$$

REFERENCES

[1] A. Kurs, A. Karalis, R. Moffatt, J. D. Joannopoulos, P. Fisher, and M. Soljačić, "Wireless power transfer via strongly coupled magnetic resonances," *Science*, vol. 317, no. 5834, pp. 83–86, 2007.

[2] S. Y. R. Hui, W. Zhong, and C. K. Lee, "A critical review of recent progress in mid-range wireless power transfer," *IEEE Trans. Power Electron.*, vol. 29, no. 9, pp. 4500–4511, Sep. 2014.

[3] J. Garnica, R. A. Chinga, and J. Lin, "Wireless power transmission: From far field to near field," *Proc. IEEE*, vol. 101, no. 6, pp. 1321–1331, Jun. 2013.

[4] L. Xiang, X. Li, J. Tian, and Y. Tian, "A crossed DD geometry and its double-coil excitation method for electric vehicle dynamic wireless charging systems," *IEEE Access*, vol. 6, pp. 45120–45128, 2018.

[5] A. Christ, M. Douglas, J. Nadakuduti, and N. Kuster, "Assessing human exposure to electromagnetic fields from wireless power transmission systems," *Proc. IEEE*, vol. 101, no. 6, pp. 1482–1493, Jun. 2013.

[6] J. Kuang, B. Luo, Y. Zhang, Y. Hu, and Y. Wu, "Load-isolation wireless power transfer with K-inverter for multiple-receiver applications," *IEEE Access*, vol. 6, pp. 31996–32004, 2018.

[7] M. Rozman, A. Ikpehai, B. Adebisi, K. M. Rabie, H. Gacanin, H. Ji, and M. Fernando, "Smart wireless power transmission system for autonomous EV charging," *IEEE Access*, vol. 7, pp. 112240–112248, 2019.

[8] T. Sasatani, C. J. Yang, M. J. Chabalko, Y. Kawahara, and A. P. Sample, "Room-wide wireless charging and load-modulation communication via quasistatic cavity resonance," *Proc. ACM Interact., Mobile, Wearable Ubiquitous Technol.*, vol. 2, no. 4, pp. 1–23, Dec. 2018.

[9] M. J. Chabalko, M. Shahmohammadi, and A. P. Sample, "Quasistatic cavity resonance for ubiquitous wireless power transfer," *PLoS ONE*, vol. 12, no. 2, Feb. 2017, Art. no. e0169045.

[10] Y. Narusue, Y. Kawahara, and T. Asami, "Maximizing the efficiency of wireless power transfer with a receiver-side switching voltage regulator," *Wireless Power Transf.*, vol. 4, no. 1, pp. 42–54, Mar. 2017.

[11] H. Hayashi, T. Sasatani, Y. Narusue, and Y. Kawahara, "Design of wireless power transfer systems for personal mobility devices in city spaces," in *Proc. IEEE 90th Veh. Technol. Conf. (VTC-Fall)*, Sep. 2019, pp. 1–5.

[12] H.-D. Lang, A. Ludwig, and C. D. Sarris, "Convex optimization of wireless power transfer systems with multiple transmitters," *IEEE Trans. Antennas Propag.*, vol. 62, no. 9, pp. 4623–4636, Sep. 2014.

[13] J. Jadidian and D. Katabi, "Magnetic MIMO: How to charge your phone in your pocket," in *Proc. 20th Annu. Int. Conf. Mobile Comput. Netw.*, Sep. 2014, pp. 495–506.
[14] L. Shi, Z. Kabelac, D. Katabi, and D. Perreault, "Wireless power hotspot that charges all of your devices," in *Proc. 21st Annu. Int. Conf. Mobile Comput. Netw.*, Sep. 2015, pp. 2–13.
[15] M. R. V. Moghadam and R. Zhang, "Multiuser wireless power transfer via magnetic resonant coupling: Performance analysis, charging control, and power region characterization," *IEEE Trans. Signal Inf. Process. Netw.*, vol. 2, no. 1, pp. 72–83, Mar. 2016.
[16] M. R. V. Moghadam and R. Zhang, "Node placement and distributed magnetic beamforming optimization for wireless power transfer," *IEEE Trans. Signal Inf. Process. Netw.*, vol. 4, no. 2, pp. 264–279, Jun. 2018.
[17] G. Yang, M. R. V. Moghadam, and R. Zhang, "Magnetic MIMO signal processing and optimization for wireless power transfer," *IEEE Trans. Signal Process.*, vol. 65, no. 11, pp. 2860–2874, Jun. 2017.
[18] W. Hua, X. Cui, H. Zhou, P. Yang, and X.-Y. Li, "Parallel feedback communications for magnetic MIMO wireless power transfer system," in *Proc. 16th Annu. IEEE Int. Conf. Sens., Commun., Netw. (SECON)*, Jun. 2019, pp. 1–9.
[19] R. Takahashi, T. Sasatani, F. Okuya, Y. Narusue, and Y. Kawahara, "A cuttable wireless power transfer sheet," *Proc. ACM Interact., Mobile, Wearable Ubiquitous Technol.*, vol. 2, no. 4, pp. 1–25, Dec. 2018.
[20] T. Sasatani, Y. Narusue, and Y. Kawahara, "Genetic algorithm-based receiving resonator array design for wireless power transfer," *IEEE Access*, vol. 8, pp. 222385–222396, 2020.
[21] K. Sumiya, T. Sasatani, Y. Nishizawa, K. Tsushio, Y. Narusue, and Y. Kawahara, "Alvus: A reconfigurable 2-D wireless charging system," *Proc. ACM Interact., Mobile, Wearable Ubiquitous Technol.*, vol. 3, no. 2, pp. 1–29, Jun. 2019.
[22] X. Zhang, S. L. Ho, and W. N. Fu, "Quantitative design and analysis of relay resonators in wireless power transfer system," *IEEE Trans. Magn.*, vol. 48, no. 11, pp. 4026–4029, Nov. 2012.
[23] C. K. Lee, W. X. Zhong, and S. Y. R. Hui, "Effects of magnetic coupling of nonadjacent resonators on wireless power domino-resonator systems," *IEEE Trans. Power Electron.*, vol. 27, no. 4, pp. 1905–1916, Apr. 2012.
[24] W. X. Zhong, C. K. Lee, and S. Y. Hui, "Wireless power domino-resonator systems with noncoaxial axes and circular structures," *IEEE Trans. Power Electron.*, vol. 27, no. 11, pp. 4750–4762, Nov. 2012.
[25] C. J. Stevens, "Magnetoinductive waves and wireless power transfer," *IEEE Trans. Power Electron.*, vol. 30, no. 11, pp. 6182–6190, Nov. 2015.
[26] B. Wang, W. Yerazunis, and K. H. Teo, "Wireless power transfer: Metamaterials and array of coupled resonators," *Proc. IEEE*, vol. 101, no. 6, pp. 1359–1368, Jun. 2013.
[27] H.-D. Lang and C. D. Sarris, "Optimization of wireless power transfer systems enhanced by passive elements and metasurfaces," *IEEE Trans. Antennas Propag.*, vol. 65, no. 10, pp. 5462–5474, Oct. 2017.
[28] H. Zhou, W. Hua, J. Deng, X. Cui, X.-Y. Li, and P. Yang, "Joint power routing and current scheduling in multi-relay magnetic MIMO WPT system," in *Proc. IEEE INFOCOM Conf. Comput. Commun.*, Jul. 2020, pp. 2283–2292.
[29] Y. Narusue, Y. Kawahara, and T. Asami, "Impedance matching method for any-hop straight wireless power transmission using magnetic resonance," in *Proc. IEEE Radio Wireless Symp.*, Jan. 2013, pp. 193–195.
[30] J. Paszkiewicz, E. Shamonina, and C. J. Stevens, "Programmable magnetoinductive devices," in *Proc. 10th Int. Congr. Adv. Electromagn. Mater. Microw. Opt. (METAMATERIALS)*, Sep. 2016, pp. 277–279.
[31] X. Shi and J. R. Smith, "Large area wireless power via a planar array of coupled resonators," in *Proc. Int. Workshop Antenna Technol. (iWAT)*, Feb. 2016, pp. 200–203.
[32] X. J. R. Shi and J. R. Smith, "Reconfigurable and adaptive coupled relay resonator platform for a moving receiver," in *Proc. Int. Workshop Antenna Technol. (iWAT)*, Mar. 2019, pp. 182–185.
[33] M. Fu, T. Zhang, P. C.-K. Luk, X. Zhu, and C. Ma, "Compensation of cross coupling in multiple-receiver wireless power transfer systems," *IEEE Trans. Ind. Informat.*, vol. 12, no. 2, pp. 474–482, Apr. 2016.
[34] J. Kim, H.-C. Son, D.-H. Kim, and Y.-J. Park, "Impedance matching considering cross coupling for wireless power transfer to multiple receivers," in *Proc. IEEE Wireless Power Transf. (WPT)*, May 2013, pp. 226–229.
[35] K. K. Ean, B. T. Chuan, T. Imura, and Y. Hori, "Impedance matching and power division algorithm considering cross coupling for wireless power transfer via magnetic resonance," in *Proc. Intelec*, Sep. 2012, pp. 1–5.
[36] F. Lemoult, N. Kaina, M. Fink, and G. Lerosey, "Wave propagation control at the deep subwavelength scale in metamaterials," *Nature Phys.*, vol. 9, pp. 55–60, Oct. 2013.
[37] F. S. Sandoval, S. M. T. Delgado, A. Moazenzadeh, and U. Wallrabe, "A 2-D magnetoinductive wave device for freer wireless power transfer," *IEEE Trans. Power Electron.*, vol. 34, no. 11, pp. 10433–10445, Nov. 2019.
[38] H. N. Bui, J.-S. Kim, and J.-W. Lee, "Design of tunable metasurface using deep neural networks for field localized wireless power transfer," *IEEE Access*, vol. 8, pp. 194868–194878, 2020.
[39] I. Khromova and C. J. Stevens, "Harnessing magneto-inductive waves for wireless power transfer," in *Proc. IEEE Wireless Power Transf. Conf. (WPTC)*, Jun. 2018, pp. 1–3.
[40] A. Hashizume, Y. Narusue, Y. Kawahara, and T. Asami, "Receiver localization for a wireless power transfer system with a 2D relay resonator array," in *Proc. IEEE Int. Conf. Comput. Electromagn. (ICCEM)*, Mar. 2017, pp. 127–129.
[41] Analog Devices. (2019). *Ltspice*. [Online]. Available: https://www.analog.com/en/design-center/design-tools-and-calculators/ltspice-simulator.html
[42] I. Awai, T. Komori, and T. Ishizaki, "Design and experiment of multi-stage resonator-coupled WPT system," in *IEEE MTT-S Int. Microw. Symp. Dig.*, May 2011, pp. 123–126.

MASAHIRO MORITA received the B.E. degree in mechano-informatics and the M.E. degree in information science and technology from The University of Tokyo, Japan, in 2018 and 2020, respectively. His studies focus on developing communication protocols for Internet of Things (IoT) systems.

TAKUYA SASATANI (Member, IEEE) received the B.E. degree in electrical and electronic engineering and the Ph.D. degree in information science and technology from The University of Tokyo, Tokyo, Japan, in 2016 and 2021, respectively. In 2017, he worked as a Lab Associate Researcher at Disney Research, Pittsburgh. He is currently a Project Assistant Professor with the Department of Electrical Engineering and Information Systems, The University of Tokyo. His studies focus on empowering the Internet of Things through exploring novel approaches for ubiquitous wireless power transfer and low-power communication systems. He is a member of ACM, IEICE, and IPSJ.

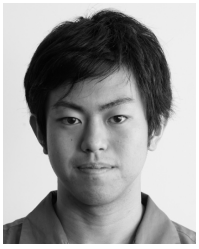

RYO TAKAHASHI received the B.E. degree in electronic and information engineering and the M.E. degree in information science and technology from The University of Tokyo, Tokyo, Japan, in 2018 and 2020, respectively, where he is currently pursuing the Ph.D. degree in electronic engineering. His research interests include wireless power transfer and digital fabrication. He is a Student Member of ACM and IEICE.

YOSHIHIRO KAWAHARA (Member, IEEE) received the B.E., M.E., and Ph.D. degrees in information and communication engineering from The University of Tokyo, Tokyo, Japan, in 2000, 2002, and 2005, respectively. In 2005, he joined the Faculty. From 2011 to 2013, he was a Visiting Scholar with Georgia Institute of Technology, Atlanta, GA, USA. He was a Visiting Assistant Professor with Massachusetts Institute of Technology, Cambridge, MA, USA, in 2013. He is currently a Professor with the Department of Electrical Engineering and Information Systems, The University of Tokyo. His research interests include computer networks and ubiquitous and mobile computing. His current research interest includes developing energetically autonomous information communication devices. He is a member of ACM, IEICE, and IPSJ.